LONGITUDINAL AND SCALAR BOSONS IN MATERIAL MEDIA AND IN VACUUM

V.S. Gorelik
Lebedev Physical Institute, Russian Academy of Sciences, Bauman Moscow State Technical University, Moscow, Russian Federation
e-mail: gorelik@sci.lebedev.ru

The article discusses properties of different type bose-particles existing in dielectric media and in vacuum. The author analyzes spectrum of lattice and excitonic polaritons for a two-atom cubic crystal and the character of dielectric function $\varepsilon(\omega)$ for transverse and longitudinal electromagnetic waves. It is demonstrated that longitudinal electromagnetic waves correspond to zero dielectric permittivity in both material media and vacuum. It is established that for certain polarization geometries during registration of Raman scattering spectra in non-centrosymmetrical crystals like gallium phosphide and lithium niobate transverse and longitudinal electromagnetic waves may be excited. The author analyzed relationship between the energy and quasi-momentum in globular photonic crystals. It is established that in such crystals the photon rest mass is non-zero and can be both positive and negative. It has been found that in dielectric and photonic crystals polariton curves have irregularities corresponding to the so-called unitary polaritons whose refraction index complies with the formula: $n^2 = 1$. The dependencies of energy on momentum for vacuum bosons corresponding to transversal, longitudinal, scalar, and pseudoscalar waves are given. It is shown that longitudinal photons in vacuum have negative effective rest mass. The author analysed conditions of observation for scalar and pseudoscalar bosons (paraphotons and axions) with extremely low rest mass ($10^{-3} \ldots 10^{-6}$ eV), which existence was predicted earlier on the base of astrophysical observations. The author examines the laws of photon-boson conversion using the intensive laser light sources as excitation radiation. The essential increase of such type conversion efficiency is predicted under the transition from spontaneous to stimulated regimes. Specific experimental installations are proposed for observation of the processes of photon-paraphoton conversion.

***Keywords*:** boson, photon, paraphoton, axion, polariton, laser, vacuum, dielectric permittivity, conversion, energy, momentum.

Introduction. Bose particles (bosons) are elementary excitations of material media and vacuum. These particles in contrast to fermions can be accumulated in quantum states in large numbers. In classical terms, a large number of bosons in a given state is equivalent to a large oscillation amplitude of the respective oscillators. Among the known bosons existing in vacuum, photons which correspond to transverse electromagnetic waves with a linear energy – momentum relationship are of particular interest: $E = c_0 p$ ($\omega = c_0 k$). Possible existence of longitudinal photons in vacuum has not yet been confirmed by any experiments and is still a matter of discussion. In the research publication [1] based on astrophysical data L.B. Okun assumes that scalar photons named paraphotons may exist in vacuum. Later, the existence of pseudoscalar bosons — axions was predicted [2]. Paraphotons and axions are the likely elementary particles of the dark matter which properties have been the subject of active research lately. The theory [3, 4] supposes that rest mass of paraphotons and axions lies within the range of $10^{-6} \ldots 10^{-3}$ eV, which corresponds to the far

infrared spectral range ($0.01 \ldots 10\,\text{cm}^{-1}$. So far a hypothesis has been made that at early stage of the Universe existence, a phase transition with formation of superstructure with a period of the order of 10^{-15} (characteristic length of weak interactions) took place. As a result of such phase transition, finite dimension clusters performing translational, respiratory, and axion oscillations were formed in vacuum. Therefore, particles analogous to acoustic and optical photons which are characteristic of complex crystal structures should exist in vacuum.

This paper analyzes properties of different types of bose-particles present in material media and in vacuum. Vacuum bosons correspond to oscillations of vacuum clusters due to softening of certain type oscillations (modes) of initial vacuum and are analogous to soft modes of crystal lattice dynamics which induce structural phase transitions in ferrielectric, ferroelastic and multiferroic materials. This article analyzes the relationship between energy and momentum (dispersion laws) for different types of bosons and processes of non-elastic interaction between them including the boson-photon conversion effect, which was analyzed before during theoretical and experimental research [3, 4].

Bosons in material media. Acoustic and optical phonons are known bosons (quasi-particles) in crystals, their spectrum being determined by the character of elastic interaction of atoms or ions forming a crystal lattice. Polar oscillations of crystal lattices cause formation of hybrid electro-mechanical waves. Respective bosons are called lattice polaritons [5, 6].

The dispersion law for polaritons in dielectric crystals is derived from the analysis of the Maxwell equation:

$$\text{rot}\vec{E} = -\frac{\partial \vec{B}}{\partial t}; \quad \text{rot}\vec{H} = -\frac{\partial \vec{B}}{\partial t}; \qquad \text{div}\vec{D} = 0; \quad \text{div}\vec{B} = 0. \tag{1}$$

Solution (1) is sought in the form of transverse and longitudinal electromagnetic waves:

$$\vec{E} = \vec{E}_0 \exp i(kr - \omega t). \tag{2}$$

In the case of cubic non-magnetic two-atom crystals for transverse polaritons the following equation holds true:

$$\text{div}\vec{D} = \varepsilon_0, \varepsilon(\omega) i(\vec{k}\vec{E}) = 0; \quad \varepsilon(\omega) = \varepsilon_\infty \frac{\omega_l^2 - \omega^2}{\omega_0^2 - \omega^2}; \quad \vec{E} \perp \vec{k}; \tag{3}$$

$$\omega^2 = \frac{c_0^2 k^2 (\omega_0^2 - \omega^2)}{\varepsilon_\infty (\omega_l^2 - \omega^2}; \quad \omega_\pm^2 = \frac{\omega_l^2 + c^2 k^2}{2} \left[1 \pm \sqrt{1 - \frac{4\omega_0^2 c^2 k^2}{(\omega_l^2 + c^2 k^2)^2}}\right]; \quad c^2 = \frac{c_0^2}{\varepsilon_\infty}.$$

Here $\varepsilon_0 = 8{,}85 \cdot 10^{-12}$; ε_∞ is high-frequency dielectric permittivity; ω_l and ω_0 are zero and pole of dielectric function $\varepsilon(\omega)$.

For longitudinal electromagnetic waves ($E \| k$) from relationship (3) it follows that $\varepsilon(\omega) = \varepsilon(\omega_l) = 0$, i.e. frequency of longitudinal electromagnetic waves for the material medium in question $\omega = \omega_l = \text{const}$.

Usually it is assumed that in vacuum $\varepsilon(\omega) = 1$. According to formula (3) it means that only the transverse waves are present. However, according to the Maxwell equation $\text{div}\vec{D} = i\varepsilon_0\varepsilon(\vec{k}\,\vec{E}) = 0$ transverse waves are present in vacuum when $\varepsilon = 0$.

Polariton waves spectrum can be analyzed experimentally by the spontaneous Raman scattering method. By selecting scattering geometry and polarization installations transverse (TO) and longitudinal (LO) polar modes can be detected. Spectra for TO and LO phonons at certain polarization geometries in gallium phosphide monocrystal with planes (100), (010) and (001) are presented in Fig. 1 [5]. Small-angle Raman scattering for a gallium phosphide sample with a plane (111) perpendicular to the the propagation direction of the exciting radiation ray allows calculating frequencies of the lower branch polaritons and plotting a dispersion curve piece in that crystal. So Raman scattering method in

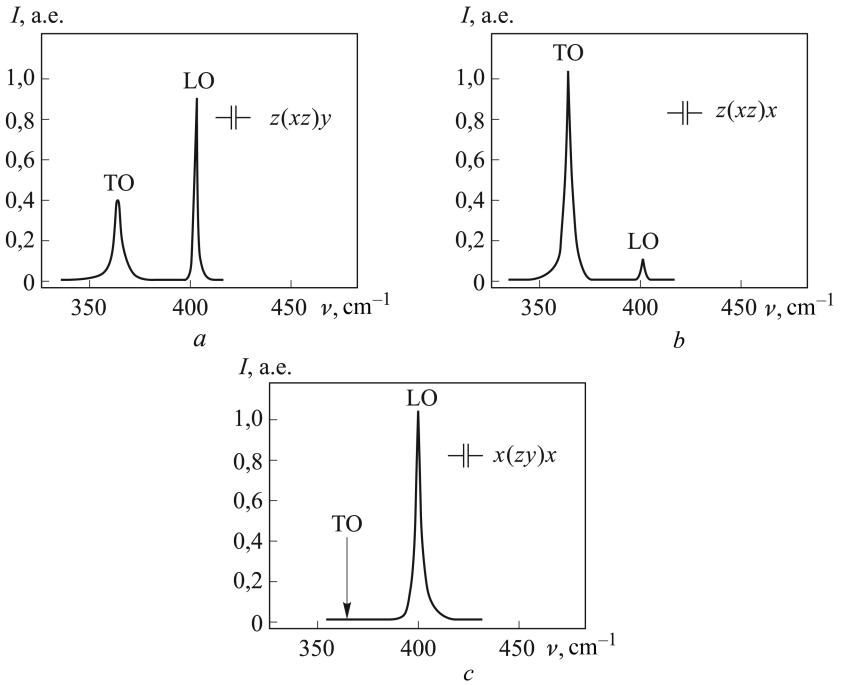

Fig. 1. Spectra of Raman scattering by longitudinal and transverse polar modes in a gallium phosphide crystal at scattering geometry $z(xz)y$ when according to the selection rules both transverse and longitudinal modes arise (*a*), at scattering geometry $z(xz)x$ when only transverse modes arise (*b*), at scattering geometry $x(zy)x$ when only longitudinal modes arise (*c*)

non-symmetrical crystals may provide conversion of photons into transverse and longitudinal lattice excitations of material media. In the case of spontaneous Raman scattering, a transformation coefficient at such a conversion is very low and constitutes approximately 10^{-6}.

In exciton spectrum band in dielectric and semiconductor crystals so called exciton polaritons or transverse and longitudinal exciton polaritons (TE, LE) are formed. When both lattice and exciton polaritons are taken into consideration in the simplest model, we arrive to the dispersion law for the transverse waves in the following form:

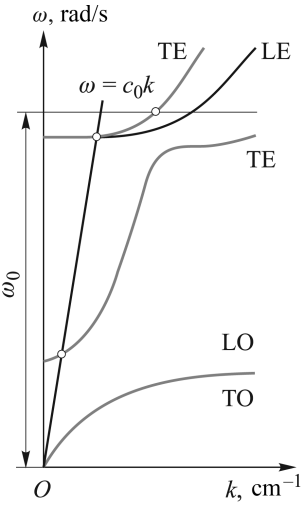

Рис. 2. Diagrammatic view of polariton curves in lattice and exiton spectrum ranges

$$\omega^2 = \frac{c_0^2 k^2}{\varepsilon(\omega)} = \frac{c_0^2 k^2 (\omega_{01}^2 - \omega^2)(\omega_{02}^2 - \omega^2)}{(\omega_{l1}^2 - \omega^2)(\omega_{l2}^2 - \omega^2)}.$$

Diagrammatic representation of the dispersion law for lattice and exciton polaritons is given in Fig. 2. When spatial dispersion is taken into account, parameters of (2) depend on a wave vector, i.e. can be expressed as the following functions:

$$\omega_{01} = \omega_{01}(k); \quad \omega_{02} = \omega_{02}(k); \quad \omega_{l1} = \omega_{l1}(k); \quad \omega_{l2} = \omega_{l2}(k).$$

Let us note that polariton curves (see Fig. 2) have irregularities corresponding to the so-called unitary polaritons for which $\omega = c_0 k$, i.e. the respective index of refraction $n = 1$.

In material media along with polar (vector) bosons, there are scalar bosons corresponding to the totally symmetrical (“respiratory”) modes. According to the selection rules, Raman scattering for scalar bosons is allowed for many molecular structures both in non-centrosymmetrical and in centrosymmetrical media. Scalar bosons correspond to the totally symmetrical oscillations of atoms (ions) in molecules and crystals, as well as to the shape oscillations of macroparticles, which constitute the material media. These modes are detected in spectra of the inelastic scattering of light in the form of additional sattelites defined by the “particular”, especially, globular light scattering.

At present, photon crystals are of particular interest for the research [7, 8], these crystals feature a superstructure with a period congruent to the visible spectrum electromagnetic wave length. In particular, globular

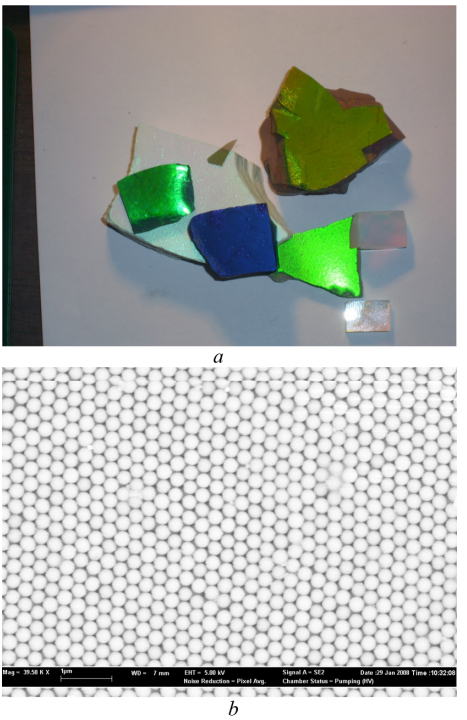

a

b

Рис. 3. Globular photonic crystals formed on the base of artificial opals (*a*) and a photografic image of surface (111) of a globular photonic crystal, obtained by the electron microscope (*b*)

photon crystals can be formed with dense packing of the dielectric balls (globules) having the same size which lies within the range of 200. . . . . 800 nm (Fig. 3). In the spectrum of the photon crystal elementary excitations, additional frequencies corresponding to "respiratory" oscillations of the globules making up the crystal. In the Raman scattering spectrum such oscillations give rise to the so-called boson peak. The analysis of the Raman scattering spectra determined by the "respiratory" modes of the globules (spectra of the "particular" light scattering) provides calculation of the frequencies for these oscillations, their damping, and distribution of the globules according to their sizes.

Dispersion curves of the electromagnetic waves derived for the globular photon crystal, having a globular size of 250 nm are presented in Fig. 4. According to the figure, the dispersion law of the electromagnetic waves in the photon crystal differs substantially from that in the vacuum one.

Dispersion curves correspond to photon-like bosons. At the same time, in the range of the small-wave vectors near the Brillouin zone boundary, the dispersion law for such bosons for the third and second dispersion branches can be approximated by the quasi-relativistic equations:

$$\omega_3^2 = \omega_0^2 + S^2k^2; \quad \omega_2^2 = \omega_0^2 - S^2k^2; \quad \omega_2^2 = \omega_{2b}^2 + c^2\chi^2; \quad \chi = \frac{\pi}{a} - k.$$

At the same time, curve *2* (see Fig. 4) features a negative index of refraction, since in this case, group and phase velocities have opposite directions. Photons in photon crystals have non-zero effective rest mass, either positive or negative. Unitary photons corresponding to the second dispersion curve (see Fig. 4) have a negative index of refraction: $n = -1$.

Papers [9–11] showed that in case of photon-photon non-harmonical oscillations which take place in non-linear optical media coupled pairs of photons — paraphotons of the material medium may be formed. After

addition of two photon spins, a paraphoton spin may be zero (which corresponds to scalar bosons) or two (which corresponds to tensor bosons). Probability of paraphoton formation in the material media increases substantially, when Fermi resonance conditions are met. In this case, in the region of the doubled frequency of the excitation radiation even-type excitons should exist.

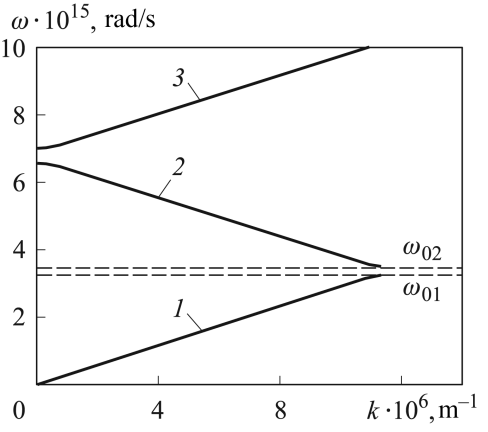

Рис. 4. Dispersion curves of the electromagnetic waves in a globular photon crystal (ω_{01}, ω_{02} – boundaries of the crystal stop-zone)

Bosons in vacuum. Papers [12–15] model physical vacuum at the early stage of the Universe existence as a quasicrystal structure made of dense packed macroparticles (maximons) having the mass $m_0 \approx 10^{-5}$ g and the size $a_0 \approx 10^{-33}$ cm and attracting to each other according to the gravitation law. The one-dimensional model of this structure is shaped as a crystal chain undergoing transverse and longitudinal oscillations in the three-dimensional space (Fig. 5, *a*). Motion equations for transverse (t) and longitudinal (l) acoustic waves of such a chain for two adjacent elements have the following form:

$$\begin{aligned} m\ddot{u}_t(p) &= -\gamma_t \left[2u_t(p) - u_t(p-1) - u_t(p+1)\right]; \\ m\ddot{u}_l(p) &= 0; \quad p = 0, 1, 2, \ldots \end{aligned} \tag{4}$$

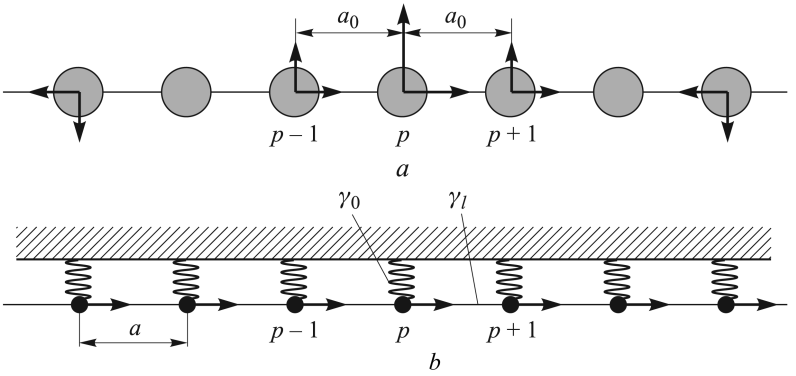

Fig. 5. Model of one-dimensional gravitational crystal chain, non-stable with respect to longitudinal acoustic waves at $a_0 \approx 10^{-33}$ cm (*a*), and a superstructure in the form of globular gravitational crystal chain at $a \approx 10^{-15}$ cm (*b*)

For solutions to equations (5) in the form of monochromatic waves

$$u_t(p) = u_t(p)_0 \exp(ikpa_0 - \omega t);$$
$$u_l(p) = u_l(p)_0 \exp(ikpa_0 - \omega t), \quad p = 0, 1, 2, \dots ,$$

the following dispersion laws of the respective waves can be derived:

$$\omega_t^2 = 4\frac{\gamma_t}{m}\sin^2\frac{ka_0}{2} = 4\frac{c_0^2}{a_0^2}\sin^2\frac{ka_0}{2}; \quad c_0^2 = \frac{\gamma_t}{m}a_0^2;$$
$$\omega_l = 0; \quad (\gamma_l = 0).$$

For small wave vectors k for transverse acoustic waves of the physical vacuum the dispersion law can be approximated by the dispersion relationship known in the theory of relativity for transverse electromagnetic waves in vacuum: $\omega_t = c_0 k$, where $c_0 = c_t$ is a velocity of transverse electromagnetic waves (velocity of light) in vacuum. With respect to the longitudinal acoustic waves, the initial phase of the physical vacuum (praphase) turned out to be non-stable ($\omega_l = 0$). Cooling of the Universe resulted in structural phase transformation and formation of superstructure with period $a \gg a_0$ ($a \approx 10^{-15}$ cm, Fig. 5, *b*). The dispersion law for transverse acoustic waves in the initial (high-temperature) phase of physical vacuum (praphase) is presented in Fig. 6, *a*.

Motion equations for translational longitudinal oscillations of the clusters in a new (low-temperature) phase take the following form:

$$M\ddot{u}_l(p) = -\gamma_0 u_l(p) - \gamma_l \left[2u_l(p) - u_l(p-1) - u_l(p+1)\right];$$

$$p = 0, 1, 2, \dots; \quad \gamma_l < 0, \quad \gamma_0 > 0.$$

A solution to equations (6) in the form of planar monochromatic waves results in the dispersion law for longitudinal optical electromagnetic waves (Fig. 6, *b*).

$$\omega_l^2 = \omega_0^2 - 4\frac{c^2}{a^2}\sin^2\frac{ka}{2}; \quad \omega_0^2 = \frac{\gamma_0}{M}; \quad \frac{c^2}{a^2} = -\frac{\gamma_l}{M}. \tag{5}$$

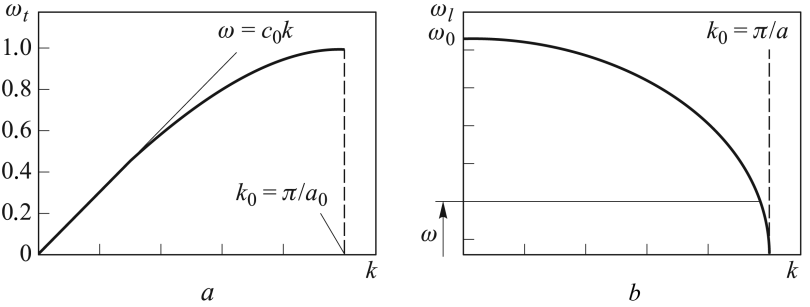

Fig. 6. Dispersion laws for transverse acoustic waves in the initial phase of physical vacuum (praphase) (*a*) and longitudinal acoustic and optical waves in vacuum after superstructural phase transformation (*b*)

Therefore, within the range of small wave vectors (continuum approximation) dispersion law (7) fulfils the relationship

$$\omega_l^2 = \omega_0^2 - c^2 k^2. \tag{6}$$

Group velocity of the waves corresponding to the dispersion law (8) can be written as follows:

$$\frac{d\omega}{dk} = -\frac{c^2 k}{\omega} = -\frac{c^2 k}{\sqrt{\omega_0^2 - c^2 k^2}}. \tag{7}$$

According to the relationship (9), in this case phase and group velocities have mutually opposite directions. Effective mass m and rest mass m_0 of the longitudinal photons according to expressions (8) and (9) are negative:

$$m = \frac{\hbar}{\dfrac{d^2\omega}{dk^2}} = -\frac{\hbar(\omega_0^2 - c^2 k^2)^{\frac{3}{2}}}{c^2 \omega^2};$$
$$m_0 = m(0) = -\frac{\hbar \omega_0}{c^2}.$$

Along with translational degrees of freedom, clusters of the low-temperature phase of vacuum have respiratory and axion degrees of freedom. Therefore, two additional dispersion branches corresponding to paraphotons and axions exist in vacuum besides the branches of the vector photons (see Fig. 6). The dispersion laws for paraphotons and axions have relativistic form:

$$\omega^2 = \omega_{par}^2 + c_0^2 k^2;$$
$$\omega^2 = \omega_{ax}^2 + c_0^2 k^2.$$

Photon-boson conversion. Generation of paraphotons, axions, and longitudinal photons in the laboratory. Quantum description of the photon-boson conversion processes in the material media and in physical vacuum is performed on the basis of introduction of Hamiltonian anaharmonical terms

$$H = H_{01} + H_{02} + V;$$
$$V = f_1 \left[a\,(a')^+ b^+ + a\,b\,(a')^+\right] + f_2 \left[a\,(a')\,b^+ + b\,a^+ (a')^+\right].$$

Here H_{01} and H_{02} are Hamiltonian functions of photon and boson fields in harmonic approximation; V is an excitation operator; a, a', b, b, a^+, $(a')^+$, b, b^+ are operators of annihilation and genesis of photon and boson fields.

Probability of the respective processes of photon-boson conversion is given by the expressions

$$W_{fi} = \frac{2\pi}{\hbar} f_1^2 \left[n_0(n'+1)(m_b+1) + n_0 m_b\,(n'+1)\right];$$

$$W_{fi} = \frac{2\pi}{\hbar} f_2^2 \left[n_0^2(m_b+1) + m_b(n_0+1)(n_0+1)\right].$$

Here n_0, n', m_b are occupation numbers for the respective fields. The energy and quasimomentum conservation laws for different elementary processes of the photon-boson conversion take the following form

$$\left\{\begin{array}{l}\hbar\omega_0 = \hbar\omega' + \hbar\omega;\\ \hbar\vec{k}_0 = \hbar\vec{k}' + \hbar\vec{k};\end{array}\right. \quad \left\{\begin{array}{l}\hbar\omega_0 + \hbar\omega = \hbar\omega';\\ \hbar\vec{k}_0 + \hbar\vec{k} = \hbar\vec{k}';\end{array}\right.$$

$$\left\{\begin{array}{l}\hbar\omega_0 = \hbar\omega'(para) + \hbar\omega(\gamma);\\ \hbar\vec{k}_0(\gamma) = \hbar\vec{k}'(para) + \hbar\vec{k}(\gamma);\end{array}\right. \quad \left\{\begin{array}{l}\hbar\omega_0 + \hbar\omega = \hbar\omega'(para);\\ \hbar\vec{k}_0(\gamma) + \hbar\vec{k}(\gamma) = \hbar\vec{k}'(para);\end{array}\right.$$

$$\left\{\begin{array}{l}\hbar\omega_0 = \hbar\omega'(axi) + \hbar\omega;\\ \hbar\vec{k}_0(\gamma) = \hbar\vec{k}'(axi) + \hbar\vec{k}(m);\end{array}\right. \quad \left\{\begin{array}{l}\hbar\omega_0 + \hbar\omega = \hbar\omega'(axi);\\ \hbar\vec{k}_0(\gamma) + \hbar\vec{k}(m) = \hbar\vec{k}'(axi);\end{array}\right.$$

$$\left\{\begin{array}{l}\hbar\omega'(axi) = \hbar\omega_0;\\ \hbar\vec{k}'(axi) = \hbar\vec{k}_0;\end{array}\right. \quad \left\{\begin{array}{l}\hbar\omega_0 = \hbar\omega'(axi);\\ \hbar\vec{k}_0(\gamma) = \hbar\vec{k}'(axi);\end{array}\right. \tag{8}$$

$$\left\{\begin{array}{l}\hbar\omega_0 + \hbar\omega_0 = \hbar\omega'(para);\\ \hbar\vec{k}_0(\gamma) + \hbar\vec{k}_0(\gamma) = \hbar\vec{k}'(para);\end{array}\right. \quad \left\{\begin{array}{l}\hbar\omega'(para) = \hbar\omega_0 + \hbar\omega_0;\\ \hbar\vec{k}'(para) = \hbar\vec{k}_0(\gamma) + \hbar\vec{k}_0(\gamma).\end{array}\right. \tag{9}$$

When excitation radiation is low ($n_0 \ll 1$), spontaneous photon-boson conversion processes take place. When the radiation is more intensive ($n_0 \gg 1$), induced processes may take place. In particular, when excitation radiation has high intensity, the induced Raman scattering takes place in the material media, when photons of the excitation radiation converse into scalar bosons of the material medium with a high transformation coefficient (≈ 0.1). Diagrams of the experimental installations used for the induced Raman scattering analysis are presented in Fig. 7 [11, 16, 17].

The induced Raman scattering spectra in calcite monocrystals, in organic compound POPOP powder, and liquid nitrogen (N_2 molecule) during the impulse laser excitation are shown in Fig. 8. In the case of nitrogen, a multi-stage conversion process takes place and both Stokes and anti-Stokes processes are registered.

Interferograms of the induced boson light scattering spectrum by the oscillations of quartz globules of both the photon crystal and spectrum of ruby laser generation with the emission line width of about 0.01 cm^{-1} produced with the help of the experimental installation presented in Fig. 7, *b*, are shown in Fig. 9. Comparison of these spectra shows that in the spectrum of the induced boson scattering there is an additional ring system corresponding to the Stokes shift $\Delta\nu \approx 0.3$ cm^{-1}.

Let us note that coherent excitation of the totally symmetrical modes (scalar bosons) during the induced Raman scattering may result in the decay of scalar ("mechanical") bosons into two entangled photons from microwave or radiowave range (the dynamic Casimir effect). Such

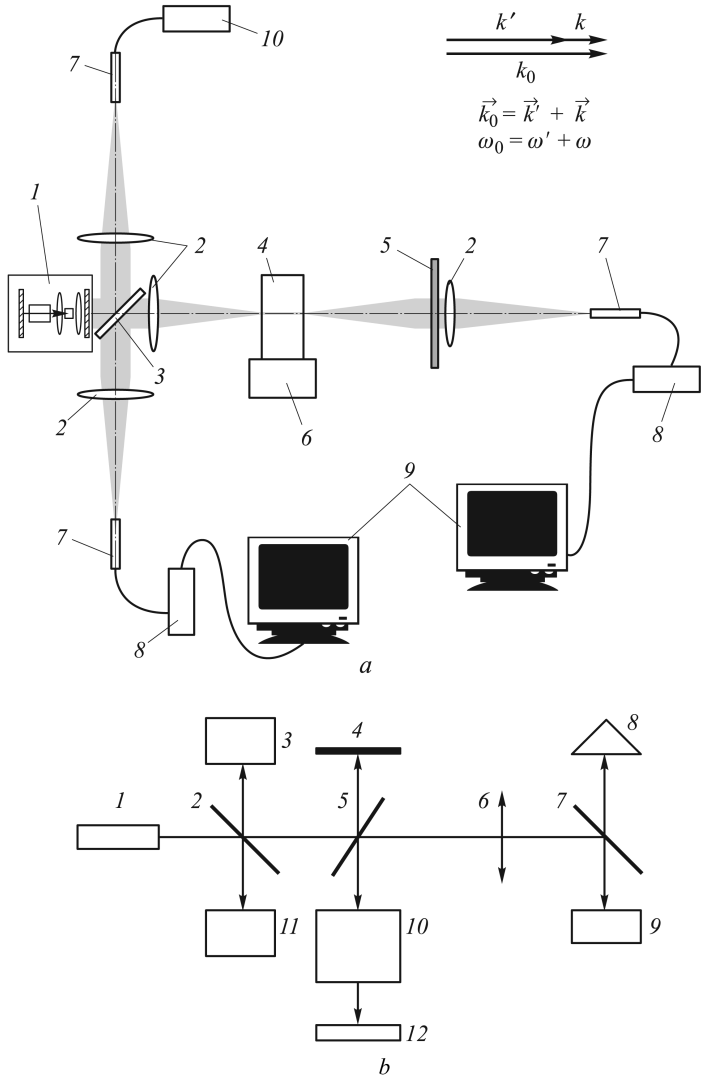

Fig. 7. Diagrams of experimental installations for the analysis of the induced Raman scattering in condensed media:
a — induced Raman scattering by molecular modes (*1* — laser; *2* — lenses; *3* — semitransparent plate; *4* — analysed sample; *5* — light filter; *6* — holder; *7* — light guide probe; *8* — minispectrometer; *9* — computer; *10* — power sensor; *b* — induced globular scattering in photon crystals (*1* — laser; *2*, *5*, *7* — semitransparent plates; *4* — light filter; *6* — lens; *3*, *8*, *11* — power sensor; *9* — analysed sample; *10* — interferometer; *12* — detector)

a process is allowed both in the centrosymmetrical and non-centrosymmetrical media and meets the conservation laws (9).

Fig. 10 shows spectra of the induced Raman scattering by transverse and longitudinal modes of a ferroelectric lithium niobate crystal placed into the ruby laser resonator generating giant pulses with a high peak intensity ($\approx 100\,\text{mW/cm}^2$). In one case, the polar axis of the crystal was directed along the laser ray (Fig. 10, *a*), in another case, it was perpendicular to the

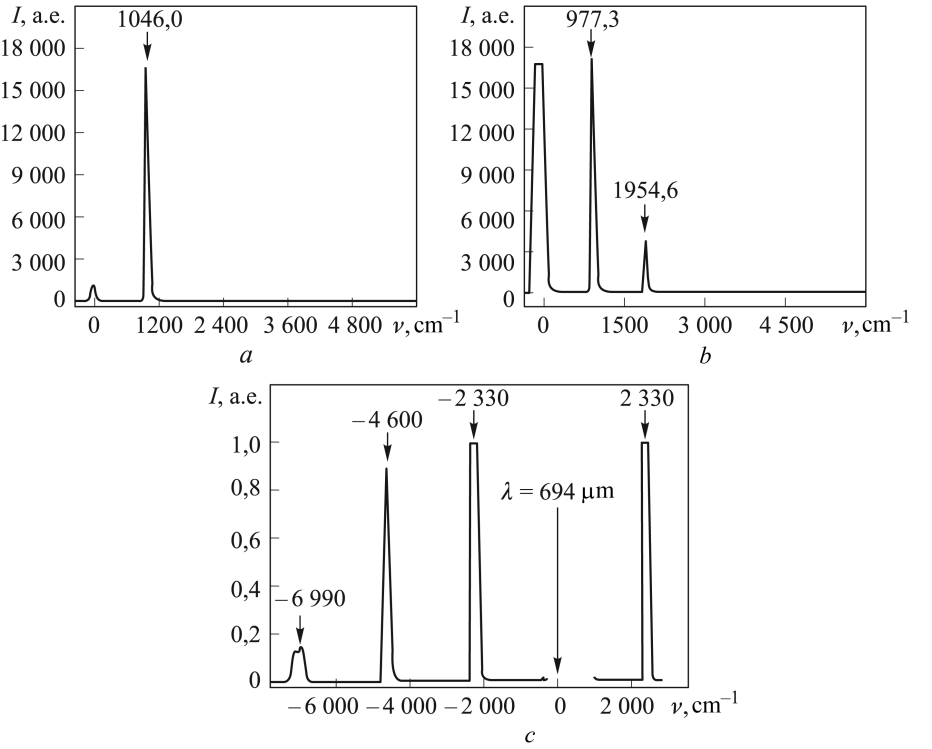

Fig. 8. Induced Raman scattering spectra of light by totally symmetrical modes in a calcite monocrystal (*a*), in organic compound POPOP powder (*b*), and liquid nitrogen (*c*)

direction of the laser impulse propagation (Fig. 10, *b*). According to the figure, the intensity of the Raman scattering is comparable to the pumping intensity. In the case of the "longitudinal" Raman scattering, the frequency shift corresponds to the longitudinal $4A_1$LO-phonon event, and in the case of the "transverse" Raman scattering, two satellites are present, one of which corresponds to a $4A_1$TO-phonon (backward scattering), and another one — to a transverse polariton (p) (forward scattering).

Fig. 11 shows a diagram of the photon-axion conversion in a magnetic field from area *a* to area *b*. Dashed line corresponds to the axions, wavy

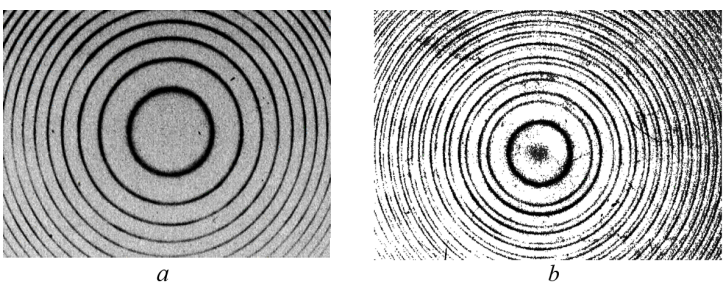

Fig. 9. Interferograms of the generation spectra of the ruby laser (*a*) and induced globular scattering of light in an artificial opal with the globule diameter of 250 nm (*b*)

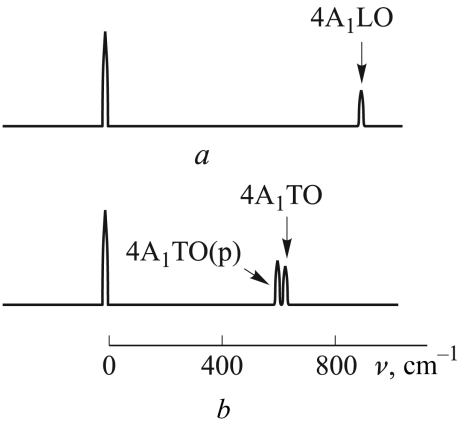

Fig. 10. Spectra of the induced Raman scattering in lithium niobate by longitudinal (*a*) and transverse (*b*) polaritons for two scattering geometries ((p) corresponds to polariton wave excitation, A_1TO corresponds to transverse polar phonon scattering)

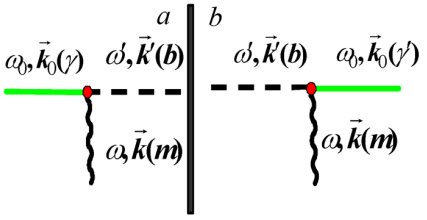

Fig. 11. Diagram of a wall penetration by light from area *a* to area *b* in the magnetic field

line corresponds to the magnetic field. Such a process (the Primakov effect) is classified as the process of a wall penetration by light. Fig. 12 shows installations for implementation of the photon-axion conversion in vacuum in a strong magnetic field, which conversion laws correspond to equations (8). Several teams of scientists have recently made experimental attempts to track this effect in vacuum [18–27]. Selection rules allow direct photon-axion conversion in a constant magnetic field in vacuum, but the probability of this spontaneous process is not high. Let us note that the use of powerful continuous wave lasers, strong magnetic field (10 Tl), and resonators in the form of interferometers (Fig. 12, *b*) did not provide a reliable signal level on the detectors used in the researches [18–27]. Thus, a reliable experimental confirmation of the effect of a wall penetration by light has not been provided so far.

Thereby, the author proposes that photon-axion and photon-paraphoton conversion should be performed not in vacuum but in a material medium. Respective synchronism conditions (energy and quasi-momentum conservation laws) for such conversion processes in a material medium could be provided by exciting radiation in the form of unitary polaritons for which the equality $n_2 = 1$ is true. As it was mentioned above, unitary polaritons are present at certain frequencies in dielectric media and in photon crystals. Experimental installations for different photon-boson conversion implementations in material media are shown in Fig. 13.

It can be assumed that in material media, the probability of photon-boson conversion should grow considerably due to photon-phonon and photon-photon interactions in dielectric media, and during the localization

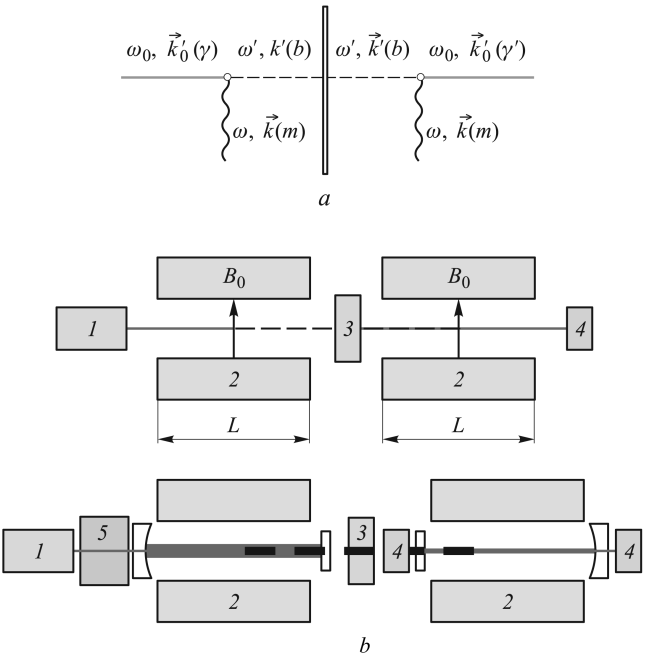

Fig. 12. Schematic diagrams of installations for photon-axion conversion in magnetic field without the additional resonator (*a*) and with Fabry-Perot resonator(*b*):
1 — laser; *2* — magnet; *3* — wall; *4* — photodetector; *5* — IO; *6* — Fabry–Perot interferometer

of the exciting laser radiation in disperse structures and in globular photon crystals.

The installations presented in Fig. 13, *a,* and *b* are designed for observation of the photon to paraphoton and inverted conversion process in the material media, when exciting radiation corresponds to unitary polaritons of the material medium. At the same time, light penetration through an opaque wall should take place. The installation shown in Fig. 13, *c* corresponds to the condition of observation of a new type of light scattering — paraphoton light scattering. During the elementary paraphoton scattering, a photon of exciting radiation decays into a paraphoton (a scalar photon) and a polar photon.

Contrary to the Raman scattering during the paraphoton scattering, according to the selection rules, they are polar modes in centrosymmetrical media such as alkali halide crystals which are active for the scattering process.

The installations shown in Fig. 13, *d* and *e* are designed for generation of THz-band infrared radiation during parametric processes and the Raman scattering. The installation shown in Fig. 13, *f* is used for detecting possible existence of longitudinal photons in vacuum.

Conclusion. This article has analyzed conditions for excitation of transverse and longitudinal electromagnetic waves both in material media

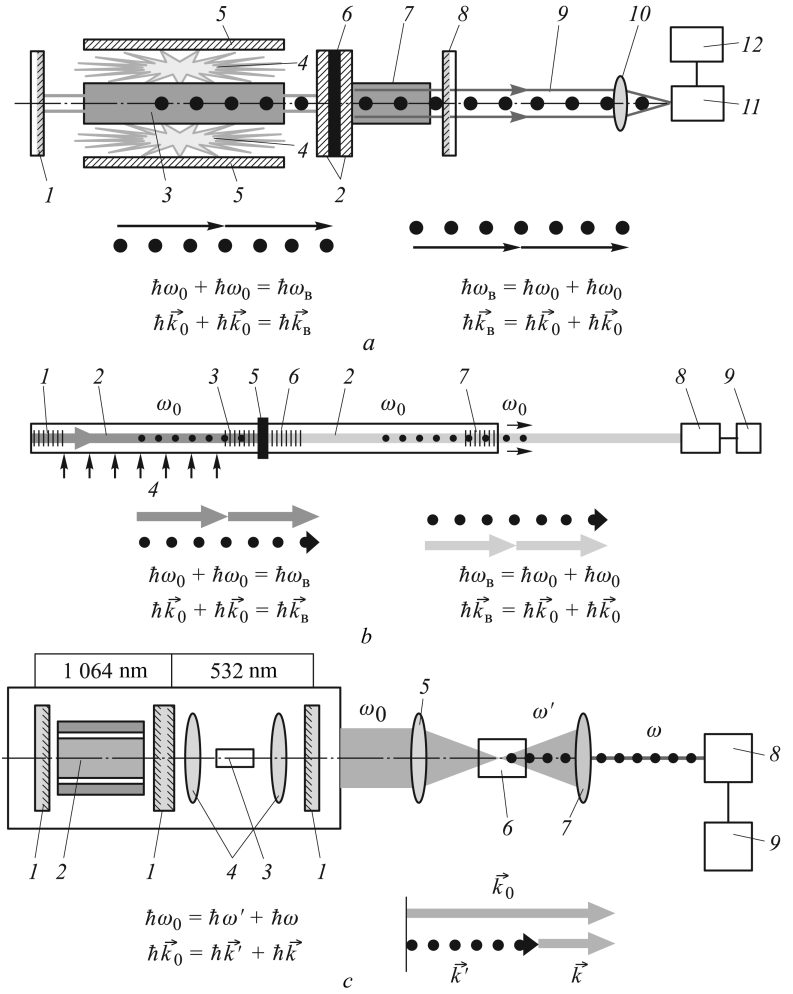

Fig. 13 (the beginning). Proposed installations for implementation of different processes of photon-boson conversion in material media:
a — for photon-paraphoton conversion in a ruby laser resonator (*1*, *2*, *8* — mirrors; *3* — active element of the ruby laser; *4* — pumping lamps; *5* — reflector; *6* — opaque wall; *7* — ruby; *9* — radiation; *10* — lens; *11*, *12* — detectors); *b* — for photon-paraphoton conversion in an erbium laser resonator (*1*, *3*, *6*, *7* — Bragg mirrors; *2* — quartz lightguide alloyed with erbium; *4* — pumping; *5* — opaque wall; *8*, *9* — detectors); *c* — for paraphoton light scattering by alkali halide crystals (*1* — mirrors; *2* — active element; *3* — nonlinear crystal; *4*, *5*, *7* — lenses; *6* — alkali halide crystal; *8*, *9* — detectors)

and in vacuum. The author has established the dispersion laws for transverse and longitudinal photons in the material media and paraphotons as well as axions in vacuum.

The author has determined conditions for optimization of photon-paraphoton conversion processes in the material media and in vacuum. It is shown that synchronism conditions for photon-paraphoton conversion in the material medium can be met, when unitary polaritons which squared refractive index is unity are used as exciting radiation.

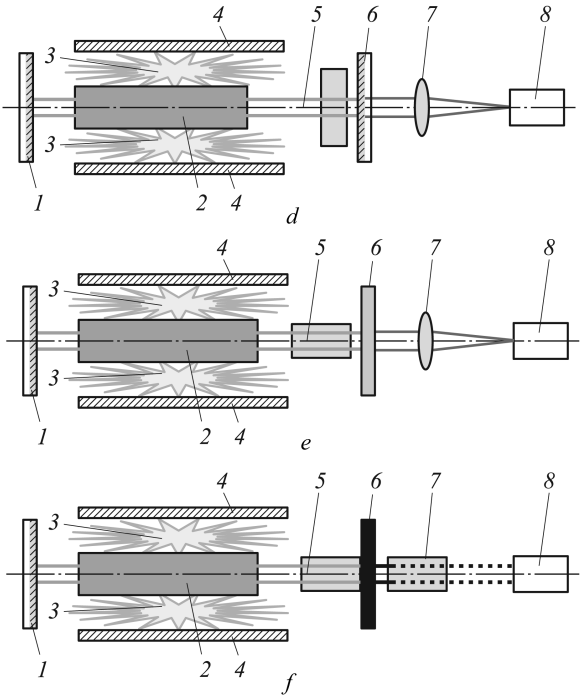

Fig. 13 (the end). *d* — for registration of infrared radiation at the induced Raman scattering by transverse polaritons in a lithium niobate crystal with the optical axis perpendicular to the direction of exciting radiation propagation (*1*, *6* — mirrors; *2* — active element; *3* — lamps; *4* — reflector; *5* — crystal; *7* — lens; *8* — detector); *e* — for registration of infrared radiation at the induced Raman scattering by longitudinal polaritons in a lithium niobate crystal having the optical axis which coincides with the direction of exciting radiation propagation (*1* — mirror; *2* — active element; *3* — lamp; *4* — shield; *5* — crystal; *6* — opaque wall; *7* — lens; *8* — detector); *f* — for registration of infrared radiation at the induced Raman scattering by longitudinal polaritons in a lithium niobate crystal (*1* — mirror; *2* — active element; *3* — lamp; *4* — shield; *5* — crystal; *6* — opaque wall; *7* — lens; *8* — detector)

The author has predicted the possibility to observe the dynamic Casimir effect during the Raman scattering by totally symmetrical oscillations of molecules and crystals as well as during the induced light scattering by bosons in globular photon crystals.

The research was supported by the Russian Foundation for Basic Research; grants 12-02-00491, 12-02-90422, 12-02-90021, 12-02-90025, 13-02-00449, 13-02-90420, 14-02-00190.

REFERENCES

[1] Okun L.B. Limits on electrodynamics: paraphotons? *Zh. Eksp. Teor. Fiz.* [J. Exp. Theor. Phys. (JETP), vol. 56, pp. 502–505], 1982, vol. 83, no. 3, pp. 892–895 (in Russ.).

[2] Hoffmann S. Paraphotons and axions: Similarities in stellar emission and detection. *Phys. Lett. B*, 1986, vol. 193, p. 117–122.

[3] Jaeckel J., Redondo J., Ringwald A. Hidden laser communications through matter — an application of MeV-scale hidden photons. *EPL (Europhysics Letters)*, 2009, EPL 87: 10010, vol. 87, no. 1, pp. 1–5. DOI:10.1209/0295-5075/87/10010

[4] Van Bibber K., Dagdeviren N.R., Koonin S.E., Kerman A.K., Nelson H.N. Proposed experiment to produce and detect light pseudoscalars. *Phys. Rev. Lett.*, 1987, vol. 59, pp. 759–762.

[5] Polivanov Yu.N. Raman scattering by polaritons. *Usp. Fiz. Nauk* [Sov. Phys.-Usp.], 1978, vol. 126, no. 2, pp. 185–232 (in Russ.).

[6] Agranovich V.M., Gartshteyn Yu.N. Spatial dispersion and negative refraction of light. *Usp. Fiz. Nauk* [Phys.-Usp.], 2006, vol. 176, no. 10, pp. 1051–1068 (in Russ.).

[7] Gorelik V.S. Optics of globular photonic crystals. *Quantum Electronics*, 2007, vol. 37, no. 5, pp. 409–432.

[8] Gorelik V.S., Shchavlev V.V. Optical devices based on materials with negative refraction. *Bull. Lebedev Phys. Inst.*, 2010, no. 12, pp. 23–32 (in Russ.).

[9] Gorelik V.S. Bound and dark photonic states in globular photonic crystals. *Acta Phys. Hung. B*, 2006, vol. 26/1–2, pp. 37–46.

[10] Gorelik V.S. Coherent and bound photonic states in globular photonic crystals. *J. of Russian Laser Research*, 2006, vol. 27, iss. 5, pp. 437–449.

[11] Gorelik V.S. Linear and nonlinear optical phenomena in nanostructured photonic crystals, filled by dielectrics or metals. *Eur. Phys. J. Appl. Phys.*, 2010, vol. 49, no. 3, pp. 33007(1)–33007(9). DOI: http://dx.doi.org/10.1051/epjap/2010014

[12] Gorelik V.S. Polaritons and their counterparts in the material and in the physical vacuum. *Proc. of Int. Sci. Meeting PIRT-2003 "Physical Interpretations of Relativity Theory"*. Moscow, 2003, pp. 56–81 (in Russ.).

[13] Gorelik V.S. Dynamics of lattice models of media and physical vacuum. *Proc. of Int. Sci. Meeting PIRT-2005 "Physical interpretations of relativity theory"*. Moscow, 2005, pp. 70–76.

[14] Gorelik V.S. Microstructure of crystalline physical vacuum and photon-boson. *Gravitation and Cosmology*, 2006, vol. 12, no. 2–3, pp. 151–154.

[15] Gorelik V.S. Dynamic of lattice models of media and physical vacuum. *Proc. of Int. Sci. Meeting PIRT-2005 "Physical interpretations of relativity theory"*. Moscow, 2005, p. 70.

[16] Tareeva M.V., Gorelik V.S., Kudryavtseva A.D., Chernega N.V. Spectral and energy characteristics of stimulated globular scattering of light. *Bull. Lebedev Phys. Inst.*, 2010, no. 11, pp. 35–41 (in Russ.).

[17] Gorelik V.S., Kudryavtseva A.D., Tareeva M.V., Chernega N.V. On generation of pulsed acoustic waves in globular photonic crystals. *Vestn. Mosk. Gos. Tekh. Univ. im. N.E. Baumana, Estestv. Nauki* [Herald of the Bauman Moscow State Tech. Univ., Nat. Sci.], 2011, no. 2(41), pp. 3–15 (in Russ.).

[18] Sikivie P., Tanner D.B., Van Bibber K. Resonantly enhanced axion-photon regeneration. *Phys. Rev. Lett.*, 2007, vol. 98. 172002(1)–172002(4). DOI: 10.1103/PhysRevLett.98.172002

[19] Andriamonje S., Aune S., Autiero D., Barth K., Belov A. An improved limit on the axion-photon coupling from the CAST experiment. *J. Cosmol. Astropart. Phys.*, 2007, iss. 4, pp. 1–23. DOI:10.1088/1475-7516/2007/04/010

[20] Chou A.S., Wester W., Baumbaugh A., Gustafson H.R., Irizarry-Valle Y., Mazur P.O., Steffen J.H., Tomlin R., Upadhye A., Weltman A., X. Yang, Yoo J. A search for chameleon particles using a photon regeneration technique. *Phys. Rev. Lett.*, 2009, vol. 102, pp. 080402(1)–080402(4). DOI: 10.1103/PhysRevLett.102.030402

[21] Pugnat P., Duvillaret L., Jost R., Vitrant G., Romanini D., Siemko A., Ballou R., Barbara B., Finger Mich., Finger Mir., Hošek J., Král M., Meissner K.A., Šulc M., Zicha J. First results from the OSQAR photon regeneration experiment: No light shining through a wall. *Phys. Rev. D.*, 2008, vol. 78, pp. 092003(1)–092003(5). DOI:10.1103/PhysRevD.78.092003

[22] Afanasev A., Baker O.K., Beard K.B., Biallas G., Boyce J., Minarni M., Ramdon R., Shinn M., Slocum P. (LIPS Collaboration). Experimental limit on optical-photon coupling to light neutral scalar bosons. *Phys. Rev. Lett.*, 2008, vol. 101, pp. 120401(1)–120401(4). DOI: 10.1103/PhysRevLett.101.120401

[23] Ahlers M., Gies H., Jaeckel J., Redondo J., Ringwald A. Laser experiments explore the hidden sector. *Phys. Rev. D.*, 2008, vol. 77, pp. 095001(1)–095001(9). DOI: 10.1103/PhysRevD.77.095001

[24] Mueller G., Sikivie P., Tanner D.B., Van Bibber K., Tanner D.B, eds. Resonantly-enhanced axion-photon regeneration. *Proc. Int. Conf. "Axions 2010"*, N.Y., American Institute of Physics, 2010, pp. 150–155. Available at: http://www.phys.ufl.edu/tanner/PDFS/Mueller10aps-reapr.pdf25 (accessed 27.05.2014).

[25] Chou A.S., Aaron S. (GammeV Collaboration). Search for chameleon particles using a photon-regeneration technique. *Phys. Rev. Lett.*, 2009, vol. 102, pp. 030402(1)–030402(4).

[26] The LIGO Scientific Collaboration & The Virgo Collaboration. An upper limit on the stochastic gravitational-wave background of cosmological origin. *Nature*, 20 august 2009, vol. 460, pp. 990–994. DOI:10.1038/nature08278

[27] Jaeckel J., Ringwald A. Search for hidden sector photons with the ADMX Detector. *Phys. Rev. Lett.*, 2010, vol. 105, pp. 171801(1)–171801(4).

The original manuscript was received by the editors on 27.05.2014

Gorelik V.S. — D. Sc. (Phys.-Math.), Professor of Physics and Mathematics, Department of Physics, Bauman Moscow State Technical University, Head of the Laboratory of Raman Scattering, Lebedev Physical Institute of the Russian Academy of Sciences, Honored Scientist of the Russian Federation, author of over 400 publications in the field of physics. Lebedev Physical Institute of the Russian Academy of Sciences, Leninskiy prospect 53, Moscow, 119991 Russian Federation.

The translation of this article from Russian into English is done by A.I. Komissarov, an engineer, a Ph.D. student, the Department of Special Machinery, Bauman Moscow State Technical University under the general editorship of I.R. Shafikova, a senior lecturer, Linguistics Department, Bauman Moscow State Technical University.